Gene Expression **2026** vol. 25(1) | e00068
DOI: 10.14218/GE.2025.00068

Original Article

Terahertz Radiation-induced Remodeling of Purine Metabolism and Membrane Raft Signaling in Human Melanoma Cells: A Metabolomic and Gene Network Analysis

Stefaniya O. Lebedeva[1], Aelita-Luiza A. Makarova[2], Ekaterina A. Butikova[3*], Nikita V. Basov[2,4], Ivan A. Razumov[1], Evgeny V. Gaisler[2], Artem D. Rogachev[2,4], Vasiliy M. Popik[5], Andrey G. Pokrovsky[2] and Vladimir A. Ivanisenko[1,6]

[1]Institute of Cytology and Genetics SB RAS, Novosibirsk, Russia; [2]A Novosibirsk State University. Institute of Medicine and Medical Technologies, Novosibirsk, Russia; [3]Research Institute of Clinical and Experimental Lymphology–Branch of the Institute of Cytology and Genetics SB RAS, Novosibirsk, Russia; [4]N. N.Vorozhtsov Novosibirsk Institute of Organic Chemistry SB RAS, Novosibirsk, Russia; [5]Budker Institute of Nuclear Physics SB RAS, Novosibirsk, Russia; [6]Novosibirsk State University, Novosibirsk, Russia

Received: August 27, 2025 | **Revised:** December 01, 2025 | **Accepted:** December 17, 2025 | **Published online:** January 26, 2026

Abstract

Background and objectives: Terahertz (THz) radiation is increasingly explored for biomedical applications, however, its non-thermal effects on cellular metabolism and regulatory networks remain insufficiently characterized. This study aimed to investigate how 2.3 THz radiation affects metabolic pathways and membrane-associated signaling in human melanoma cells.

Methods: SK-MEL-28 melanoma cells were exposed to 2.3 THz radiation for 45 min using the 1st Novosibirsk free-electron laser. Cell viability was assessed by 3-(4,5-dimethylthiazol-2-yl)-2,5-diphenyltetrazolium bromide and trypan blue assays. Metabolic alterations were detected by targeted metabolomics using liquid chromatography–tandem mass spectrometry. Gene network analysis was performed using the ANDSystem platform to reconstruct gene and protein interaction networks linking altered metabolites to membrane receptors, lipid raft proteins, and signaling pathways. Overrepresentation analysis of biological processes was applied to identify enriched functional categories.

Results: THz exposure did not affect cell viability but induced significant alterations in purine metabolism, pantothenate/CoA biosynthesis, and the pentose phosphate pathway. Network analysis revealed that these metabolic changes were associated with membrane raft reorganization and receptor-mediated signaling involving epidermal growth factor receptor and G-protein subunits. Additional effects were observed in pathways related to chromatin organization and post-translational regulation.

Conclusions: THz radiation induces coordinated remodeling of metabolic and regulatory networks in melanoma cells without cytotoxicity. These findings highlight the role of membrane-associated signaling in mediating THz-induced cellular responses and provide insight into potential biomedical applications of THz technologies.

Keywords: Terahertz radiation; Metabolomic analysis; Cell membrane; Melanoma cell; Gene network analysis; Purine metabolism.

***Correspondence to:** Ekaterina A. Butikova, RICEL-branch of the IC&G, Timakova str.2., 630090, Russia. ORCID: https://orcid.org/0000-0002-0619-4278. Tel: +7-952-937-39-47, E-mail: katabutikova@gmail.com

How to cite this article: Lebedeva SO, Makarova A-LA, Butikova EA, Basov NV, Razumov IA, Gaisler EV, *et al*. Terahertz Radiation-induced Remodeling of Purine Metabolism and Membrane Raft Signaling in Human Melanoma Cells: A Metabolomic and Gene Network Analysis. *Gene Expr* 2026;25(1):e00068. doi: 10.14218/GE.2025.00068.

Introduction

Terahertz (THz) radiation refers to electromagnetic waves with frequencies ranging from 0.1 to 10 THz (~3 mm to 100 μm), lying between the infrared and microwave regions of the electromagnetic spectrum.[1] Due to its expanding applications in pharmaceutical technologies,[2] civil security systems,[3] and biomedical research,[4] interest in its biological effects has grown substantially. THz radiation can exert both thermal and non-thermal effects depending on power and exposure conditions.[5–7] Under non-thermal conditions, pulsed THz radiation interacts with biomolecules without measurable heating, suggesting specific molecular and structural

© 2026 The Author(s). This article has been published under the terms of Creative Commons Attribution-Noncommercial 4.0 International License (CC BY-NC 4.0), which permits noncommercial unrestricted use, distribution, and reproduction in any medium, provided that the following statement is provided. "This article has been published in *Gene Expression* at https://doi.org/10.14218/GE.2025.00068 and can also be viewed on the Journal's website at https://www.xiahepublishing.com/journal/ge".

responses.[8] Thermal effects are primarily associated with high-power millimeter-wave sources, whereas pulsed THz exposures produce negligible heating.[9,10] Non-thermal mechanisms may involve linear or nonlinear resonances at the molecular level; for instance, local disruption of hydrogen bonds in DNA may lead to altered gene expression.[11]

On the one hand, most of the commonly used THz radiation intensities are not harmful to cells and do not reduce their viability. This has been confirmed in a study on human dermal fibroblasts, where no signs of apoptosis or oxidative stress were observed.[12] On the other hand, there are reports of THz-induced adipogenic differentiation of mesenchymal stem cells, as well as indications that THz radiation may influence gene transcription.[13] In addition, a research group led by Dr. Peltek has been actively studying the effects of THz radiation on a range of biological objects, including *E. coli*,[14,15] *G. icigianus*,[16] and human embryonic stem cells,[17] under exposure to a frequency of 2.3 THz.

Contemporary studies indicate that cell membranes are a primary target of THz radiation. In HeLa cells, exposure to 0.10–0.29 THz increased lateral lipid diffusion and induced an order–disorder transition in the bilayer under non-thermal conditions.[18] In HT22 neuronal cells, continuous-wave 0.1 THz irradiation enhanced membrane permeability and facilitated transmembrane transport of small molecules.[19] These findings are consistent with the underlying physics: phospholipid bilayers and their hydration shells support collective motions in the THz band, and THz spectroscopy detects a long-range hydration layer extending approximately four to five water layers beyond the membrane, providing a direct physical coupling between THz fields and the lipid–protein matrix.[20] Similar effects have been demonstrated under exposure to radiation with a wavelength of 130 μm, which may induce reversible impairments in the barrier properties of neuronal membranes.[21] Previously, we reported alterations in the metabolic profile after a 45-min exposure of SK-MEL-28 tumor cells to THz radiation, with no signs of cytotoxicity but with metabolomic and bioinformatic evidence of changes in mitochondrial membrane rafts.[22] These observations support the concept that membranes and their lipid rafts might act as primary sensors of THz radiation, mediating subsequent metabolic and regulatory responses.

Metabolomics is a field of bioanalytical chemistry aimed at studying biological systems, which enables comprehensive monitoring of metabolic pathways and their responses to various stimuli.[23] It enables the identification of pathway-level changes and the discovery of adaptive mechanisms underlying cellular responses. By integrating metabolomic data with gene network reconstruction, it is possible to connect metabolite-level changes to regulatory processes at the protein and signaling levels.[24] The ANDSystem software platform is an automated bioinformatics tool that reconstructs molecular interaction networks from biomedical databases and scientific literature using ontology-based knowledge extraction.[25–27] This approach has been successfully applied in various studies to identify molecular mechanisms of pathological processes and to interpret omics data.[28–30] In our previous study on THz-irradiated melanoma cells, ANDSystem revealed strong connectivity between mitochondrial membrane proteins and enzymes involved in purine metabolism.[22]

The aim of the present study was to analyze high-performance liquid chromatography (HPLC)–tandem mass spectrometry (MS/MS) metabolomic data of SK-MEL-28 melanoma cells exposed to 2.3 THz radiation for 45 min, identify key metabolic pathways affected, and determine the role of membrane rafts in regulating these THz-induced metabolic and signaling changes.

Materials and methods

Cell culture

Cells (SK-MEL-28) were seeded two days before irradiation. Cells were cultured in T-25 flasks (TPP, Switzerland) (n = 5) in DMEM/F12 (1:1) medium supplemented with L-glutamine (Biolot, Russia), 10% fetal bovine serum (Hyclone, New Zealand), and gentamicin at a concentration of 50 μg/mL (Dalchimpharm, Russia). Incubation was carried out at 37°C in a humidified atmosphere containing 5% CO_2. Cells were seeded at a density of 4.0×10^4 cells/cm^2 (1×10^6 per flask) and reached approximately 1.2–1.6 $\times 10^5$ cells/cm^2 (3–4 $\times 10^6$ per flask) by the time of irradiation, in 5 mL of culture medium to ensure uniform exposure across the monolayer surface (90–93%).

Cell viability and 3-(4,5-dimethylthiazol-2-yl)-2,5-diphenyltetrazolium bromide (MTT) assays

Cell viability was assessed 72 h after THz exposure. Cells from both control and irradiated groups were detached from the substrate using a trypsin–versene solution (1:1) (Biolot, Russia), after which 0.4% trypan blue solution (Applichem, Germany) was added to the resulting cell suspension. The numbers of viable and necrotic cells were determined using a Countess automated cell counter (Invitrogen, USA) in accordance with the manufacturer's instructions. Cell survival 72 h after irradiation was assessed using the MTT assay. Cells were seeded into 96-well plates at a density of 1×10^4 cells per well, with five replicates for each experimental point. After 72 h, 20 μL of the phenazine methosulfate-based reagent (Cell Titer 96® AQueous One Solution, Promega, USA) was added to 100 μL of culture medium in each well. Incubation was carried out under standard conditions for 4 h. Optical density was measured at 490 nm using a Multiskan SkyHigh Microplate Spectrophotometer (Thermo Fisher, USA).

THz-irradiation

THz irradiation was carried out at the Novosibirsk Free Electron Laser (NovoFEL) facility of the Budker Institute of Nuclear Physics, SB RAS. THz radiation was generated at a wavelength of 130 μm (2.3 THz). The power density of the radiation was 0.056 W/cm^2. The total irradiation time for each sample was 45 min. The irradiation scheme and methodology are shown in Figure 1. All parameters of the THz laser are outlined in Table 1.[31]

Sample preparation for HPLC–MS/MS analysis

Metabolomic analysis was carried out using five independent biological replicates (n = 5), each analyzed in two technical replicates to ensure reproducibility. Prior to sample preparation, cells were collected as a suspension, and their concentration was determined using a Countess automated cell counter (Invitrogen). Based on the obtained data, a suspension volume corresponding to 1×10^6 cells was transferred into 1.5 mL tubes. Centrifugation was performed at 1,000 g for 5 min. The supernatant was removed, and the cell pellet was resuspended in 1 mL phosphate-buffered saline. After a second centrifugation under the same conditions, phosphate-buffered saline was removed, and 100 μL of Milli-Q water was added to the pellet. The samples were thoroughly mixed until complete resuspension, frozen, and stored at −80°C until analysis. Before analysis, the samples were thawed at room temperature and normalized to contain 1×10^6 cells per 100 μL of Milli-Q water. To disrupt membrane structures, two cycles of freezing (−70°C) and thawing at room temperature were performed, followed by sonication using a 25 kHz ultrasonic system

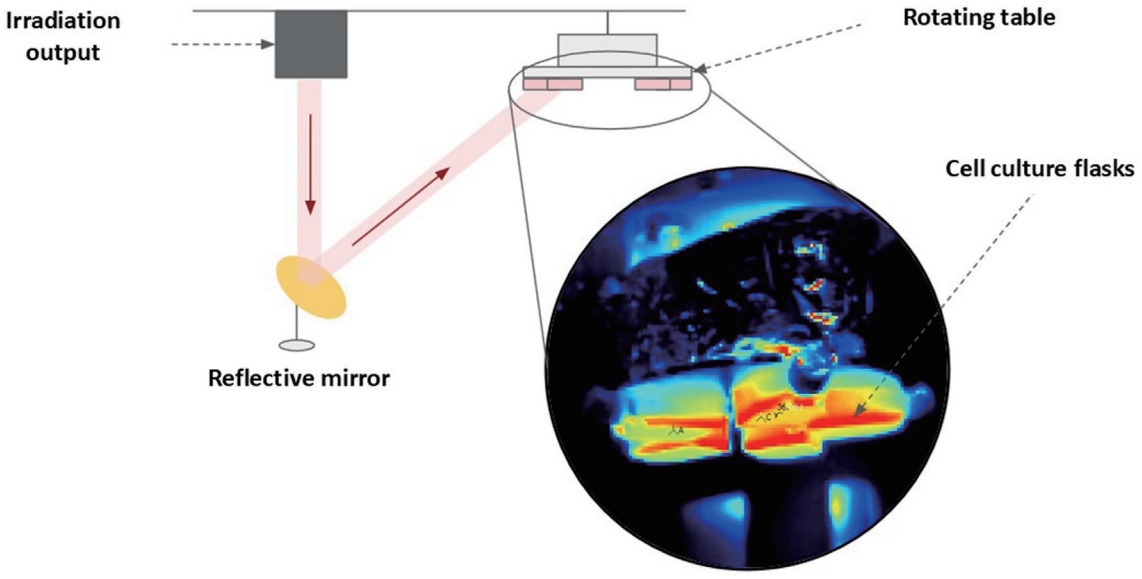

Fig. 1. Scheme of the cell irradiation setup at the Novosibirsk Free Electron Laser (Budker Institute of Nuclear Physics, SB RAS). Terahertz irradiation was performed at a wavelength of 130 µm. Each experiment was conducted using five biological replicates (n = 5).

(model Elma Sonic S30H, Germany) at room temperature for 5 min. Then, 400 µL of pre-cooled methanol/acetonitrile mixture (1:1, v/v) was added to the resulting lysate. Extraction was carried out on a thermoshaker at 22°C, 900 rpm for 20 min, followed by centrifugation at 4°C and 16,000 g for 15 min. The obtained supernatant was transferred into vials and subjected to HPLC–MS/MS analysis. Each sample was analyzed in two analytical replicates. The detailed extraction and HPLC–MS/MS protocol was previously described in our publication.[32]

HPLC

Chromatographic separation was performed on an LC-20AD Prominence system (Shimadzu, Kyoto, Japan) equipped with an SIL-20AC autosampler (Shimadzu, Japan) thermostated at 10°C. Eluent A consisted of 5% acetonitrile in an aqueous solution of 20 mM $(NH_4)_2CO_3$, adjusted to pH 9.8 with aqueous ammonia. Eluent B was 100% acetonitrile. Each sample was analyzed twice, namely in hydrophilic interaction liquid chromatography and reversed-phase chromatography modes. The hydrophilic interaction liquid chromatography gradient was as follows: 0 min – 98% B, 2 min – 98% B, 6 min – 0% B, and 10 min – 0% B. The column was then re-equilibrated for 4 min. The reversed-phase chromatography gradient was as follows: 0 min – 0% B, 1 min – 0% B, 6 min – 98% B, and 16 min – 98% B. The column was then re-equilibrated for 3 min. The flow rate for both methods was 300 µL/min. The injection volume was 10 µL. Separations in both chromatographic modes were conducted using a monolithic column based on 1-vinyl-1,2,4-triazole, 2 × 60 mm. The monolithic column material was synthesized according to the procedure described in reference[33]: copolymerization was carried out in a glass tube with an internal diameter of 2 mm using a monomer mixture of styrene/divinylbenzene/1-vinyl-1,2,4-triazole taken at a volume ratio of 10:50:40, respectively.

Table 1. The main parameters of the 1st Novosibirsk Free Electron Laser[31]

Parameter	Value
Frequency, THz; wavelength, µm	3.3–0.75 (90–400)
Pulse repetition frequency, MHz	5.64
Pulse duration, ps	100
Average power, kW	0.5
Peak power, MW	1
Spectrum width, %	<1%

kW, kilowatts; MHz, megahertz; MW, megawatts; Ps, picoseconds; THz, terahertz.

Mass spectrometry

Metabolite detection was performed in multiple reaction monitoring mode in both positive and negative ion modes using an API 6500 QTRAP mass spectrometer (AB SCIEX, USA) equipped with an electrospray ionization source. The main mass spectrometric parameters were as follows: ion source voltage 5,500 V for positive and −4,500 V for negative ionization; desolvation gas temperature, 475°C; collision gas, "high"; nebulizer gas, desolvation gas, and curtain gas pressures, 33, 33, and 30 psi, respectively. Declustering potential was ±91 V, entrance potential ±10 V, and collision cell exit potential ±9 V. The multiple reaction monitoring dwell time was 3 ms. Instrument control and data acquisition were carried out using Analyst 1.6.3 software (AB SCIEX). Precursor-to-fragment ion transitions, metabolite names, fragmentation times, and corresponding collision energies were adapted from reference.[34]

Gene network reconstruction

To reconstruct the gene networks, regulatory pathways were considered between significantly altered metabolites and two types of their regulators, human cellular receptors and lipid raft proteins. Human enzymes involved in the transformation of identified metabolites were retrieved from the KEGG Pathway database (https://www.genome.jp/kegg/pathway.html) by querying their KEGG compound identifiers to obtain associated metabolic pathways.[35] Only human pathways (prefix "hsa") were considered. The analy-

Table 2. Schemes of template regulatory molecular–genetic pathways between enzymes and cellular receptors, as well as lipid raft proteins of human cells

№	Template schematic description
1	Cellular receptors – protein–protein interactions → enzymes. Lipid rafts – protein–protein interactions → enzymes
2	Cellular receptors – regulation of activity/degradation/proteolysis/post-translational modifications (PTMs)/transport → enzymes. Lipid rafts – regulation of activity/degradation/proteolysis/PTMs/transport → enzymes
3	Cellular receptors – regulation of activity/degradation/proteolysis/PTMs/transport → human proteins – regulation of activity/degradation/proteolysis/PTMs/transport → enzymes. Lipid rafts – regulation of activity/degradation/proteolysis/PTMs/transport → human proteins – regulation of activity/degradation/proteolysis/PTMs/transport → enzymes
4	Cellular receptors – protein–protein interactions → human proteins – protein–protein interactions → enzymes. Lipid rafts – protein–protein interactions → human proteins – protein–protein interactions → enzymes

sis included enzymes directly catalyzing reactions involving the target metabolite, as well as those involved in one upstream and one downstream reaction step. KEGG compound identifiers of identified metabolites were extracted from the HMDB database (https://hmdb.ca/).[36] The list of cellular receptors was obtained from the RaftProt database (https://raftprot.org/).[37] The list of cellular receptors was extracted from the CellTalkDB database (http://tcm.zju.edu.cn/celltalkdb/browser.php?list=receptors).[38] The ANDSystem cognitive platform with its graphical interface ANDVisio was used to reconstruct and analyze gene networks. Using the "Pathway Master" module of the ANDVisio program,[25–27] the regulatory molecular–genetic pathways were constructed. UniProt identifiers of cellular receptors, raft proteins, and enzymes were explicitly submitted to the "Pathway Master" query. Types of molecular interactions, including protein–protein interactions, regulation of protein activity, degradation, transport, post-translational modifications, cleavage, and catalytic reactions, were ticked as parameters in the interaction filter. The object "human proteins" for templates 3 and 4 was passed implicitly to the query. ANDVisio automatically extracted interactions between objects from the ANDSystem knowledgebase according to the templates in Table 2. The templates describe such relationships between proteins as protein–protein interactions, regulation of activity, degradation, transport, post-translational modifications, proteolysis, and catalytic reactions.

Gene network analysis

For templates No. 1 and No. 2, manual verification of connections was performed to exclude errors arising from automated text analysis by the ANDSystem. For templates No. 3 and No. 4, no additional filtering steps were applied, as these templates yielded only the most highly connected proteins. Using ANDVisio, statistical analysis of the gene network was conducted, in which the topological properties of the network were examined based on the degree centrality of graph vertices. Degree centrality is defined as the ratio of the number of connections of a given vertex to the total number of other vertices in the network. This measure makes it possible to assess how strongly a particular vertex is connected to the rest of the network.

A Python 3.11 script incorporating Pandas 2.2.3 and Matplotlib 3.9 was used to calculate the number of regulatory connections for each vertex in each of the regulatory pathway templates and visualize the histograms.

The overrepresentation analysis of Gene Ontology biological processes within the gene network was conducted using the DAVID web tool (https://david.ncifcrf.gov/tools.jsp).[39] UniProt IDs of the gene network participants were uploaded to the DAVID Functional Annotation Tool. The analysis was conducted with Benjamini-Hochberg multiple comparison correction and a significance threshold of 0.05. The data on ages of the gene network participants and overrepresented Gene Ontology biological processes were obtained from the GenOrigin Database (http://genorigin.chenzxlab.cn/).[40] The Age Coefficient for each overrepresented biological process (OBP) was calculated as the ratio of the average age of the gene network participants within the OBP to the average age of all genes annotated in the OBP.

Statistical analysis

Statistical tests were conducted with Python 3.11 using its SciPy 1.15.0 stats module. Metabolome coverage of the analytical approach was assessed using Student's t-test. Significantly altered metabolomic profiles were revealed through analysis of the experimental data using the Mann–Whitney U test with multiple-testing correction (Benjamini–Hochberg procedure).

Overrepresentation analysis of metabolic processes was conducted using the MetaboAnalyst 6.0 web tool (https://www.metaboanalyst.ca/).[41] For the participants of the reconstructed gene networks, statistically significant biological processes (adjusted *P*-value, or *q*-value < 0.05) were identified using the DAVID web tool (DAVID knowledgebase version: v2024q1).

Results

Cell viability and MTT assay

After 72 h, both groups were subjected to the MTT assay to assess cell survival; the results are presented in Table 3. As shown in Table 3, the survival rate of the experimental group was high (87–89%) and comparable to that of the control.

Metabolomic screening by HPLC–MS/MS

A total of 40 statistically significant metabolites were identified whose levels changed in cells exposed to THz radiation (Table 4).

Table 3. Cell viability and MTT assay results for a 45-min exposure evaluated 72 h post-irradiation

Group	THz-45	IR-45	Control-45
Cell viability (%)	96.6 ± 1.2	93.4 ± 1.7	97.6 ± 0.8
MTT assay (OD)	87.1 ± 3.2	97.7 ± 5.7	100.0 ± 2.7

Data are presented as mean ± SE. Experimental groups: THz (terahertz irradiation), IR (infrared irradiation), and Control. Each group included five independent biological replicates (n = 5). MTT results are expressed as % of control. MTT, 3-(4,5-dimethylthiazol-2-yl)-2,5-diphenyltetrazolium bromide; OD, optical density; SE, standard error.

Table 4. Metabolites significantly altered by THz irradiation relative to the control group

Metabolites and changes in their levels			
Increase (↑)			Decrease (↓)
Purine metabolism	**Lipid metabolism**	**Energy metabolism**	**Purine and related metabolites**
Uracil*	Cardiolipin (18:2/18:2/18:2/22:6)	Gluconic acid	Adenosine monophosphate (AMP)*
7-methylguanine*	Ceramide (d18:1/16:1 OH)	Malic acid	1-methyladenine*
Deoxyinosine*	Ceramide (d18:1/16:2)	Glyceric acid	Adenosine*
Inosine triphosphate (ITP)*	Ceramide (d18:1/16:0)	Adenylsuccinic acid	Adenine*
Hypoxanthine*	Ceramide (d18:1/18:1)	Salicyluric acid	Deoxyguanosine diphosphate (dGDP)*
Xanthine*	Ceramide (d18:1/24:1)	1-methylnicotinamide	Methylcysteine
7-methylguanosine*	Phosphatidylcholine (16:0/20:4)	N-acetylglucosamine	5-hydroxyindoleacetic acid (5-HIAA)
Guanine*	Phosphatidylcholine (16:0/22:6)	N-oleoylethanolamine	Cytidine diphosphate (CDP)*
Cytosine*	Phosphatidylcholine (38:5)	Acadesine	
Anthranilate	Phosphatidylcholine (40:6)	Histamine	
Dephospho-CoA	Aminoimidazole carboxamide ribonucleotide (AICAR)		

*Purine metabolism-related metabolites are denoted by an asterisk. THz, terahertz.

The *P*-values for these metabolites are provided in Supplementary Table 1.

A list of metabolic pathways with varying levels of significance was obtained, from which the pathways with *P*-value < 0.05 were selected (Fig. 2, Table 5).

Reconstruction and analysis of gene networks

We hypothesized that THz radiation affected the supramolecular structures of lipid rafts as well as the signaling pathways originating from cellular receptors. Absorption of radiation by lipid rafts may have led to their enlargement or disintegration, as well as to changes in their localization on the membrane surface. An electromagnetic pulse acting on large receptor structures may have triggered signaling pathways that were not normally activated under physiological conditions.

Within this hypothesis, we reconstructed gene networks regulating enzymes through two types of regulators, cellular receptors and lipid raft proteins. Gene networks were constructed using the "Pathway Master" module of the ANDVisio program. Database queries were generated according to the templates presented in Table 1.

Gene networks of enzyme regulation by cellular receptors

Template 1, representing protein–protein interactions between

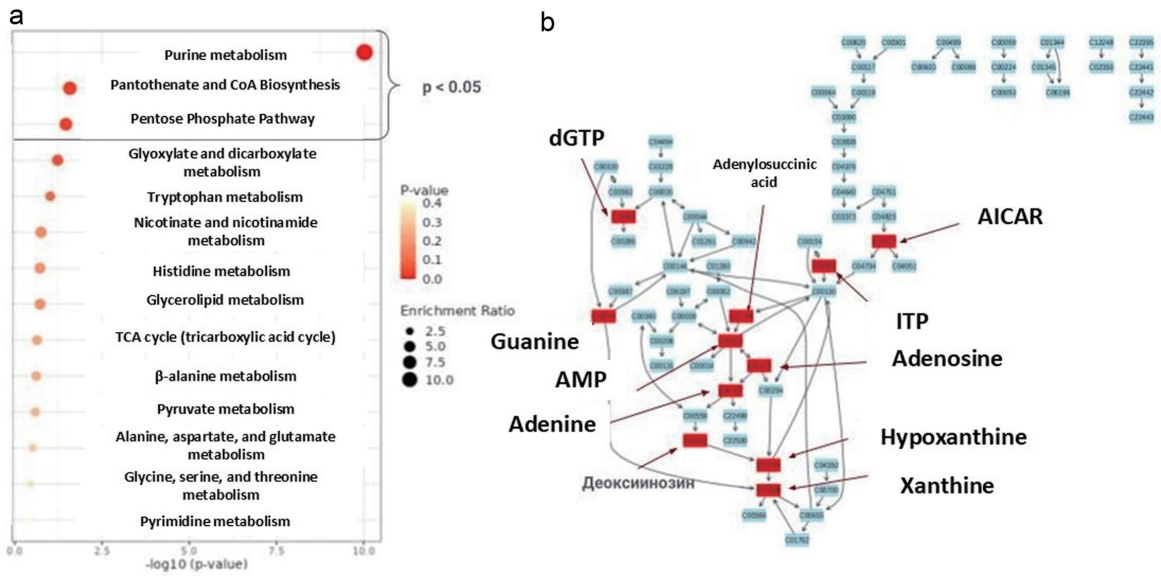

Fig. 2. THz-induced alterations in metabolic pathways. (a) Overrepresented metabolic processes; (b) Purine metabolism pathway. AICAR, 5-aminoimidazole-4-carboxamide riboside; AMP, adenosine monophosphate; dGTP, deoxyguanosine triphosphate; ITP, inosine triphosphate; THz, Terahertz.

Table 5. Annotated metabolic pathways

Metabolic pathway	The level of significance (*p*-value)
Purine metabolism	9.47×10^{-11}
Pantothenate and CoA biosynthesis	2.65×10^{-2}
Pentose phosphate pathway	3.45×10^{-2}

enzymes and cellular receptors, was combined with Template 2, describing the regulation of enzyme biological functions (Fig. 3). The resulting gene network included 30 enzymes and 73 cellular receptors, with 118 protein–protein interaction links, 4 links of protein activity regulation, 2 catalytic links, and 2 proteolysis links.

In the gene network obtained by combining Templates 1 and 2, we highlighted enzymes catalyzing reactions involving guanine. According to the metabolomic analysis, guanine levels were increased in the group of cells after THz irradiation. The gene network reconstructed by combining Templates 1, 2, 3, and 4 was too extensive for visual representation; instead, a quantitative analysis of the regulatory influences from cell receptors to enzymes was performed for it (Fig. 4).

The histogram in Figure 4 illustrates the number of regulatory influences from cellular receptors to the 25 most highly regulated enzymes involved in the biosynthesis and degradation of significant metabolites.

Gene network of enzyme function regulation by lipid raft proteins

To construct the gene network of enzyme regulation by lipid raft proteins, Template 1 (representing protein–protein interactions) was combined with Template 2 (describing the regulation of enzyme biological functions by lipid raft proteins) (Fig. 5). The resulting gene network included eightenzymes and nine lipid raft proteins, with eight protein–protein interaction links and three links of protein degradation regulation.

In the gene network in Figure 5, we identified key lipid raft proteins: ALBU, PL4, and PGK1. In addition, by combining Templates 1, 2, 3, and 4, a large gene network was constructed (not shown in the paper), for which a quantitative analysis of the regulatory influences from lipid rafts to the enzymes was performed. The histogram in Figure 6 illustrates the number of regulatory connections from lipid raft proteins to the 25 most strongly regulated enzymes participating in the biosynthesis and degradation of key metabolites.

Overrepresentation analysis of biological processes

Overrepresentation analysis of biological processes was performed using the DAVID web tool. For the gene network of enzyme regulation by cellular receptors, 577 OBPs were identified, among which we highlighted processes of chromatin organization regulation, G protein–related signaling pathways, and regulation of post-translational modifications. For the gene network of enzyme regulation by lipid rafts, 91 OBPs were identified, includ-

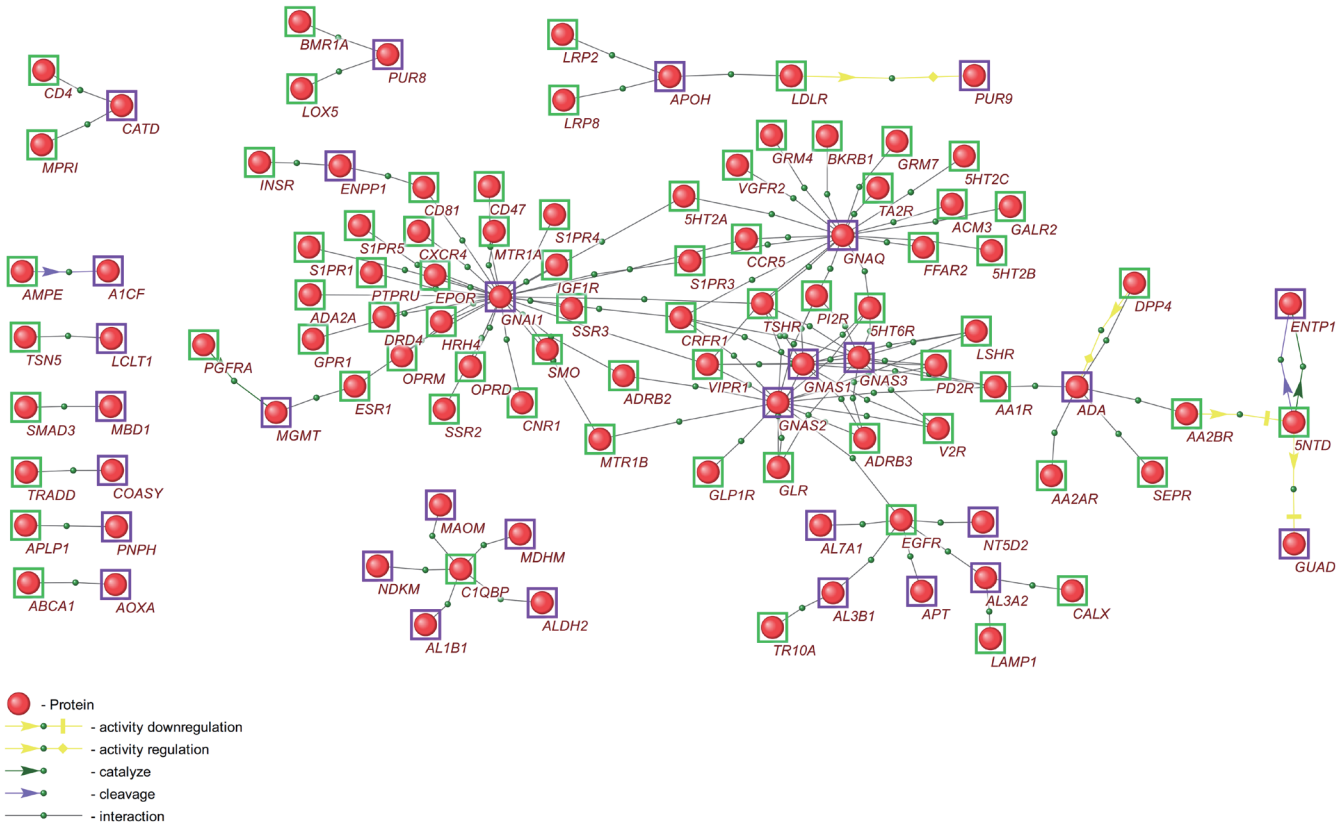

Fig. 3. Gene network of enzyme function regulation by cellular receptors. The enzymes of metabolite conversion are purple-framed spheres. Green-framed spheres represent cellular receptors.

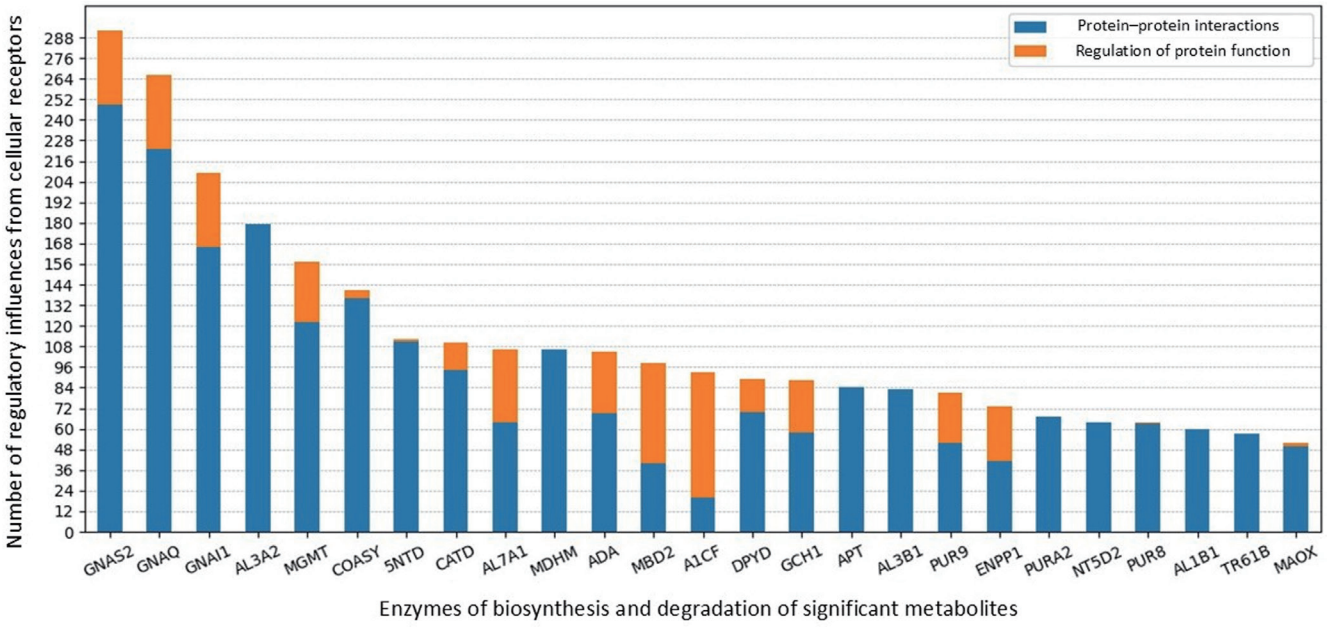

Fig. 4. Histogram of the distribution of regulatory influences on enzymes from cellular receptors.

ing G protein–related signaling pathways, chromatin organization regulation, and protein post-translational modification processes.

Discussion

The lack of cytotoxicity under prolonged exposure is, in our view, an expected outcome, since Wilmink *et al*.[42] demonstrated that differences between irradiated groups at a frequency of 2.52 THz in human dermal fibroblast cells and the sham-control group were not statistically significant. It was also shown that exposure to THz radiation at three different frequencies (1.4 THz, 2.52 THz, 3.11 THz) in human keratinocytes resulted in cell viability that did not differ significantly from the sham-control.[43]

Human neural progenitor cells were irradiated for 30 min with

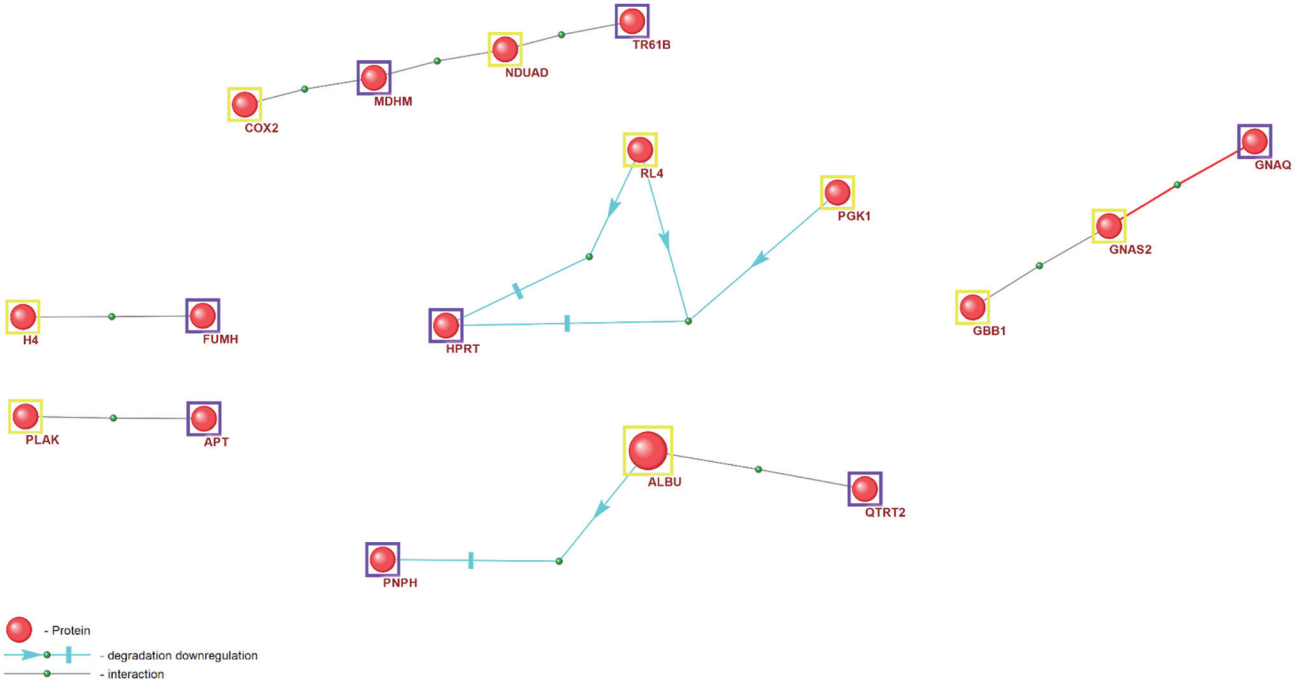

Fig. 5. Gene network of enzyme function regulation by lipid raft proteins. Purple-framed spheres represent the enzymes of metabolite conversion. Yellow-framed spheres denote lipid raft proteins.

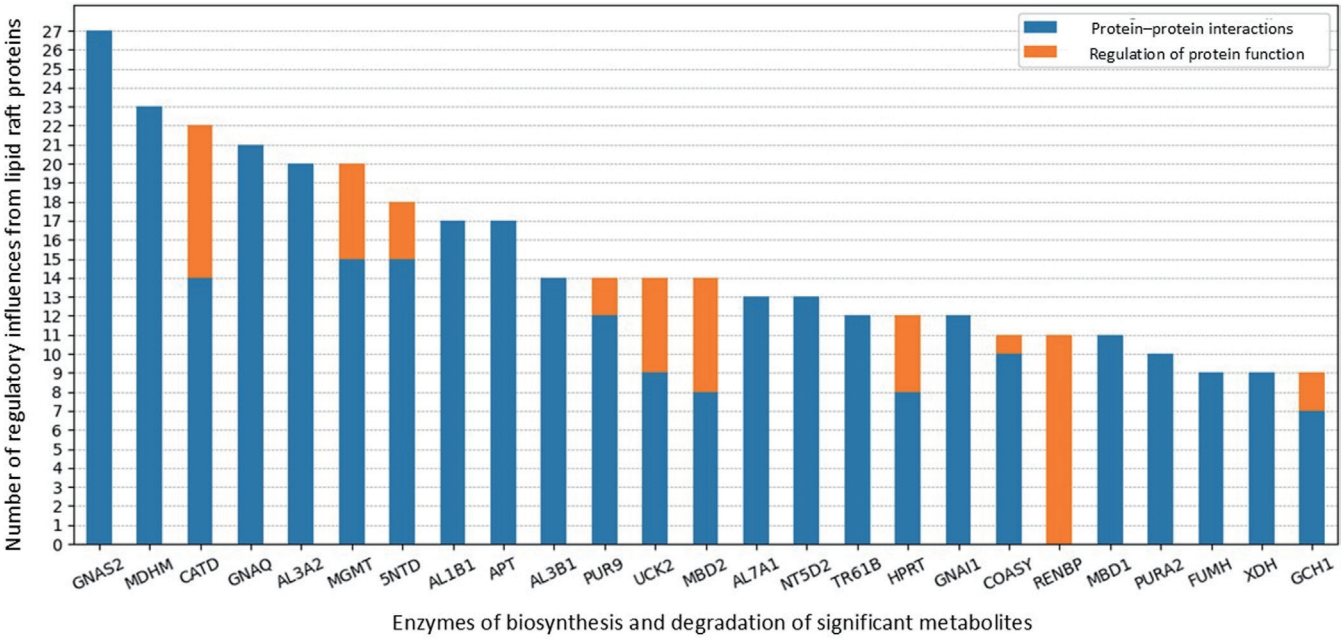

Fig. 6. Histogram of the distribution of regulatory influences on enzymes from lipid raft proteins.

pulsed THz radiation at 100 Hz. The study demonstrated no changes in proliferative activity following THz exposure in cultures of both healthy and tumor cells (neuroblastoma).[44]

In another study, broadband THz radiation (0.05–1.2 THz) at powers of 30, 2, and 0.1 μW was shown to have no substantial effect on mitochondrial functional activity in either adherent cell cultures (human lung carcinoma A-549, human breast adenocarcinoma BT-20, human colon carcinoma COLO 320 HSR), suspension cultures (NMC-1, human histiocytic leukemia U937, human promyelocytic leukemia HL-60), or primary cultures (thymocytes and splenocytes of CBA mice).[45] Importantly, no disruption of the integrity of their bilipid surface membranes was observed.

These findings confirm that THz exposure does not induce significant cytotoxicity, thereby allowing investigation of subtle metabolic and signaling rearrangements without confounding effects of cell death.

One of the most distinct and pronounced metabolomic changes observed after 45 min of irradiation was a decrease in adenine levels accompanied by an increase in hypoxanthine, inosine triphosphate, and deoxyinosine. Such shifts are characteristic of a transition from *de novo* synthesis to the purine salvage pathway,[46] which is more energy-efficient and indicates an adaptive cellular response to THz radiation. In the reconstructed gene network, adenosine deaminase (ADA) forms five direct protein–protein interactions with membrane receptors; these interactions represent physical contacts, meaning that the enzyme is "recruited" to the plasma membrane and operates in close proximity to receptor complexes. Such localization is optimal for rapid processing of extracellular adenosine as well as the intracellular deoxyadenosine pool, consistent with the metabolomic profile.

Dipeptidyl peptidase-4 (DPP4) is known as an anchoring protein on the surface of immune and tumor cells: binding increases the catalytic constant of ADA and stabilizes it on the membrane.[47] The most significant interaction was the DPP4–ADA pair. We hypothesize that DPP4 activation under THz exposure accelerates adenine/adenosine deamination, producing hypoxanthine/inosine, thereby restarting the salvage cascade through hypoxanthine-guanine phosphoribosyltransferase and inosine monophosphate dehydrogenase, shifting the cell to a more "cost-efficient" nucleotide resynthesis mode.[48] Moreover, the DPP4–ADA complex is localized in lipid rafts, where the co-receptor CD45 forms a signaling metaplex, leading even to raft domain redistribution.[49] Thus, secondary utilization of purines reduces the cellular demand for adenosine triphosphate (ATP) and amino acids, which is consistent with both the absence of pronounced cytotoxicity and the increase in the AMP-activated protein kinase marker 5-aminoimidazole-4-carboxamide ribonucleotide. In addition, decreased adenosine and adenine levels prevent accumulation of S-adenosylhomocysteine, a methyltransferase inhibitor, thereby providing a "window" for cellular energy landscape reorganization without the risk of hypermethylation. At the same time, studies on the demethylating potential of THz radiation open the hypothesis that, in melanoma, such demethylation may have both pro- and anti-tumor effects depending on the specific loci. This rearrangement should therefore be interpreted as an adaptive and non-thermal response to THz stress.

Gene network analysis also revealed that the hexameric receptor complement component 1 Q subcomponent-binding protein (C1QBP, also known as p32/HABP1) formed five direct protein–protein interactions with enzymes of the tricarboxylic (TCA) acid cycle and oxidative catabolism—monoamine oxidase B (MAOM (MAO-B)), malate dehydrogenase 2 (mitochondrial) (MDHM (MDH2)), aldehyde dehydrogenase 1 family member B1 (ALDH1B1), aldehyde dehydrogenase 2 (mitochondrial) (ALDH2), and the mitochondrial nucleoside diphosphate kinase (NME4/NDKM). C1QBP is known to form high-stoichiometry complexes with MDH2 and ALDH2, stabilizing them at the inner membrane and increasing electron transfer efficiency to Complex I.[50] Metabolomic analysis showed elevated malic and glyceric acid levels, consistent with enhanced activity of the malate–aspartate shuttle catalyzed by MDH2. Increased ITP and deoxyinosine further point to activation of the ATP-independent salvage pathway (via NME4), which is energetically advantageous under conditions of enhanced respiration.

In addition to purine metabolism, THz exposure also influenced pantothenate/CoA biosynthesis and the pentose phosphate pathway. Both pathways are closely linked to energy and redox regulation. Enhanced CoA biosynthesis may indicate an increased demand for acyl-group transfer and mitochondrial oxidation, while activation of the pentose phosphate pathway supplies NADPH for antioxidant defense and anabolic reactions. Together, these alterations suggest that THz irradiation induces a coordinated metabolic response aimed at maintaining redox balance and energetic stability under non-thermal electromagnetic stimulation.

The receptor–ubiquitin ligase 5′-nucleotidase domain containing 2 (5NTD (NT5DC2)) reportedly proteolytically cleaves ectonucleoside triphosphate diphosphohydrolase 1 (ENTP1) while simultaneously inhibiting guanine deaminase activity. This combination of effects explains the accumulation of ITP and the decrease in guanine.

The guanine nucleotide-binding protein, alpha stimulating activity polypeptide 2 (GNAS2 (Gas)), and guanine nucleotide-binding protein, alpha q polypeptide (GNAQ (Gaq)) proteins receive the largest number of inputs from plasma membrane receptors in the gene network. Notably, p32 and Gα proteins colocalize within membrane domains, and their convergence during THz-induced raft rearrangement may activate two possible signaling cascades: (1) the cyclic adenosine monophosphate/protein kinase A signaling pathway (cAMP/PKA via Gas), leading to phosphorylation of the MDH2/ALDH2 complex; and (2) the phospholipase C–inositol trisphosphate–calcium signaling pathway (PLC–IP3–Ca^{2+} via Gaq), causing activation of the mitochondrial calcium uniporter and an additional influx of NADH.[51] Both cascades accelerate TCA cycle activity and explain the excess production of malic acid.

A study on the effect of THz radiation on the proteome of the thermophilic bacterium Geobacillus icigianus demonstrated changes in the expression of numerous proteins after 15 min of exposure to THz radiation generated by a free-electron laser.[16] Alterations were observed in electron transport chain components, regulators of transcription, translation, DNA repair, cell growth, and chemotaxis, as well as in pathways of peptidoglycan synthesis, riboflavin, NAD, FAD, and pyridoxal phosphate biosynthesis, TCA cycle metabolites, and ATP biosynthesis, indicating a rapid cellular response to THz radiation.

The gene network of cellular responses to THz radiation revealed that epidermal growth factor receptor (EGFR) and a group of Gα subunits formed the densest cluster of interactions with enzymes processing guanine/adenine-containing metabolites. THz-induced rearrangement of lipid rafts may have promoted ligand-independent EGFR clustering, consistent with previous reports demonstrating that EGFR can undergo membrane-driven clustering and activation in response to non-chemical physical perturbations, independent of ligand binding.[52] In the network, EGFR was connected to APT, ALDH7A1, NT5D2, and GNAS2. These enzymes govern the terminal steps of IMP/XMP reutilization and the glycerol shunt; thus, their spatial proximity to EGFR provides the cell with a "short" metabolic loop for rapid replenishment of the nucleotide pool.

GNAI1, GNAQ, and GNAS-short isoform (GNAS2) were identified as high-degree nodes (11 to 29 receptors). Through these, receptors from adrenergic, purinergic, lysophosphatidic acid, and other families can transactivate EGFR (the so-called GPCR–RTK transactivation). The GNAS family elevates intracellular cAMP levels, and increased cAMP has already been shown to trigger expression of several salvage pathway enzymes (e.g., APRT, PNP).[53] In essence, Gα nodes act as a "gateway": the higher the density of GPCR inputs, the stronger the shift from *de novo* synthesis toward purine salvage, which in our experiments was reflected as increased hypoxanthine, ITP, and deoxyinosine levels, accompanied by decreased adenine.

The most highly organized structures of the plasma membrane, as well as of mitochondria, are lipid rafts. Lipid rafts are dynamic nanoscale assemblies of sphingolipids, cholesterol, and proteins that can stabilize and coalesce into larger platforms.[54] A key function of lipid rafts is signal transduction, particularly the regulation of metabolic processes. Albumin (regulator) inhibits the degradation of purine nucleoside phosphorylase (hereinafter referred to as PNPH), which catalyzes the phosphorolytic cleavage of the N-glycosidic bond in deoxyadenosine, a metabolite whose levels increased in the metabolomic profiles of cells exposed to THz laser irradiation.[55] According to our calculations, the enzymes GNAS2 and MDHM are influenced by the largest number of corresponding lipid raft proteins through protein–protein interactions. THz-induced "compaction" of rafts increases the affinity of the ALBU→PNPH interaction and shifts the cell toward deoxyadenosine degradation.

The OBPs we identified are consistent with those reported by other authors studying the effects of THz radiation on cells. Exposure to THz radiation at the molecular level can lead to changes in the regulation of chromatin organization, G protein–related signaling pathways, and post-translational modifications. In a study,[6] THz radiation was shown to affect chromatin organization and gene expression in microbial and eukaryotic cells, suggesting possible mechanisms of non-thermal action of THz radiation. Thus, THz radiation of appropriate intensity and frequency can induce epigenetic changes such as histone modifications,[56] altered binding conditions of methylated DNA, or DNA demethylation, ultimately leading to changes in gene expression and chromatin structure. This is particularly relevant to cancer therapy, where demethylation can be used to suppress oncogenes.[57]

A large body of research has focused on aberrant DNA methylation in melanoma.[58,59] Melanoma is one of the most promising cancer types for biomedical applications of THz radiation in therapy due to the easy accessibility of malignant lesions. Manipulating DNA methylation to correct alterations in tumors may become an effective strategy for molecular cancer therapy.

THz radiation may also induce conformational changes in chromatin, influencing its compactness and accessibility for transcription and DNA repair.[6] In addition to van der Waals interactions, THz radiation can affect hydrogen bonds that stabilize chromatin structure, leading to either decondensation or condensation.[60]

The OBPs we identified are also consistent with the findings of a study, which reported that THz radiation can influence neuronal morphology and dynamic properties, inducing nonlinear resonance effects in proteins that may, in turn, impact chromatin organization and signaling pathways.[21]

The results obtained show that both the gene network of enzyme regulation by cellular receptors and the network associated with lipid rafts include numerous OBPs. This indicates a complex interplay between these elements and their significance in cellular physiology. The identified processes may serve as a basis for further research in molecular biology and medicine. The study highlights the need for continued analysis of interactions between different signaling pathways and their impact on cellular functions.

Limitations

This study was performed using a single human melanoma cell line, SK-MEL-28, and therefore the observed effects may reflect

cell-type-specific responses. Further validation across additional cellular models and tissue systems is required to confirm the generality of the identified mechanisms. A commercial infrared lamp with predefined parameters was used as a control to exclude non-specific thermal and THz-independent effects; the detected metabolites should not be considered markers of infrared exposure itself.

The present work focused exclusively on the cytoplasmic membrane and its associated proteins, proposing a mechanistic link between THz-induced membrane perturbations, mitochondrial activity, and metabolic regulation. These interpretations represent a theoretical model based on metabolomic and network data and should be further tested experimentally. Future studies involving other THz frequencies, exposure regimes, and broader molecular targets will be essential to clarify the universality and biophysical basis of these proposed mechanisms.

Conclusions

Exposure of SK-MEL-28 melanoma cells to 2.3 THz radiation produces coordinated alterations in metabolic and regulatory networks without affecting cell viability. Metabolomic profiling reveals pronounced modulation of purine metabolism, pantothenate/CoA biosynthesis, and the pentose phosphate pathway, while bioinformatic analysis links these changes to processes of chromatin organization, G-protein–mediated signaling, and post-translational regulation. Gene network reconstruction indicates that lipid raft–associated receptors and enzymes act as central mediators of these responses, suggesting that cellular membrane proteins may serve as sensitive interfaces for THz irradiation perception and transduction. The observed remodeling of nucleotide and energy metabolism suggests an adaptive, non-thermal reprogramming of biochemical pathways, enabling cells to maintain homeostasis under electromagnetic stimulation.

Acknowledgments

The authors would like to acknowledge the Center for Genetic Resources of Laboratory Animals at the Institute of Cytology and Genetics SB RAS for providing the cell lines and equipment necessary for conducting cellular assays. The authors are grateful to the group at the Budker Institute of Nuclear Physics SB RAS for providing terahertz generation.

Funding

HPLC-MS/MS analysis was conducted with the support of state project No. FSUS-2025-0012. Cultivation and cell counting were supported by budget project No. FWNR-2022-0023. The experimental part of the study was carried out with the support of the Russian Science Foundation (Project No. 19-72-202) at the unique Novosibirsk Free Electron Laser installation using equipment from the Siberian Center for Synchrotron and Terahertz Radiation. The authors also thank state project No. 075-00365-25-00 of N.N. Vorozhtsov Novosibirsk Institute of Organic Chemistry of the Siberian Branch of the Russian Academy of Sciences for providing resources. The preparation of monolithic columns for HPLC was conducted with the support of state project No. FWUR-2024-0032. Bioinformatics analysis was carried out within the framework of budget project FWNR-2022-0020. The authors acknowledge support from the state assignment of RICEL – a branch of IC&G SB RAS, project No. FWNR-2025-0016.

Conflict of interest

The authors have no conflict of interest related to this publication.

Author contributions

Study concept and design (LSO, MALA, BEA, BNV, RAD, PVM, IVA), acquisition of data (LSO, MALA, BEA, BNV), analysis and interpretation of data (MALA, BEA, BNV, RIA), drafting of the manuscript (LSO, BEA), critical revision of the manuscript for important intellectual content (RIA, GEV, RAD, PVM, IVA), administrative, technical, or material support (PVM, PAG, IVA). All authors have made significant contributions to this study and have approved the final manuscript.

Ethical statement

The human melanoma cell line SK-MEL-28 (ATCC HTB-72), obtained from the collection of the Center for Genetic Resources at the Laboratory Animal Center of the Institute of Cytology and Genetics SB RAS (Novosibirsk, Russia), was used in this experiment. The experiments did not involve human participants, human tissue samples, or primary human cells. Therefore, ethical approval and informed consent were not required.

Data sharing statement

The data that support the findings of this study are publicly available.

References

[1] Yang X, Zhao X, Yang K, Liu Y, Liu Y, Fu W, *et al*. Biomedical Applications of Terahertz Spectroscopy and Imaging. Trends Biotechnol 2016;34(10):810–824. doi:10.1016/j.tibtech.2016.04.008, PMID:27207226.

[2] Wallace VP, Taday PF, Fitzgerald AJ, Woodward RM, Cluff J, Pye RJ, *et al*. Terahertz pulsed imaging and spectroscopy for biomedical and pharmaceutical applications. Faraday Discuss 2004;126:255–63, discussion 303-11. doi:10.1039/b309357n, PMID:14992411.

[3] Tzydynzhapov G, Gusikhin P, Muravev V, Dremin A, Nefyodov Y, Kukushkin I. New Real-Time Sub-Terahertz Security Body Scanner. J Infrared Millim Terahertz Waves 2020;41(6):632–641. doi:10.1007/s10762-020-00683-5.

[4] Son JH, Oh SJ, Cheon H. Potential clinical applications of terahertz radiation. J Appl Phys 2019;125(19):190901. doi:10.1063/1.5080205.

[5] Mattsson MO, Zeni O, Simkó M. Is there a Biological Basis for Therapeutic Applications of Millimetre Waves and THz Waves? J Infrared Millim Terahertz Waves 2018;39(9):863–878. doi:10.1007/s10762-018-0483-5.

[6] Fëdorov VI, Serdyukov DS, Cherkasova OP, Popova SS, Nemova EF. The influence of terahertz radiation on the cell's genetic apparatus. J Opt Technol 2017;84(8):509–514. doi:10.1364/jot.84.000509.

[7] Cherkasova OP, Serdyukov DS, Nemova EF, Ratushnyak AS, Kucheryavenko AS, Dolganova IN, *et al*. Cellular effects of terahertz waves. J Biomed Opt 2021;26(9):090902. doi:10.1117/1.JBO.26.9.090902, PMID:34595886.

[8] Alexandrov BS, Rasmussen KØ, Bishop AR, Usheva A, Alexandrov LB, Chong S, *et al*. Non-thermal effects of terahertz radiation on gene expression in mouse stem cells. Biomed Opt Express 2011;2(9):2679–2689. doi:10.1364/BOE.2.002679, PMID:21991556.

[9] Wang M, Yang G, Li W, Wu Q. An overview of cancer treatment by terahertz radiation. In: 2013 IEEE MTT-S International Microwave Workshop Series on RF and Wireless Technologies for Biomedical and Healthcare Applications (IMWS-BIO); 2013 Dec 9-11; Singapore. IEEE; 2013. p. 1–3. doi:10.1109/IMWS-BIO.2013.6756170.

[10] Wilmink GJ, Rivest BD, Roth CC, Ibey BL, Payne JA, Cundin LX, *et al*. In vitro investigation of the biological effects associated with human dermal fibroblasts exposed to 2.52 THz radiation. Lasers Surg Med 2011;43(2):152–163. doi:10.1002/lsm.20960, PMID:20740621.
[11] Zaytsev KI, Dolganova IN, Chernomyrdin NV, Katyba GM, Gavdush AA, Cherkasova OP, *et al*. The progress and perspectives of terahertz technology for diagnosis of neoplasms: A review. J Opt 2020;22(1):013001. doi:10.1088/2040-8986/ab4dc3.
[12] Cherkasova O, Surovtseva M, Lykov A, Kazakov O, Kabakov A, Poveshchenko O, *et al*. Studying the effect of 0.14 THz radiation on human dermal fibroblasts. AIP Conf Proc 2019;2098(1):020004. doi:10.1063/1.5098148.
[13] Bock J, Fukuyo Y, Kang S, Phipps ML, Alexandrov LB, Rasmussen KØ, *et al*. Mammalian stem cells reprogramming in response to terahertz radiation. PLoS One 2010;5(12):e15806. doi:10.1371/journal.pone.0015806, PMID:21209821.
[14] Peltek S, Meshcheryakova I, Kiseleva E, Oshchepkov D, Rozanov A, Serdyukov D, *et al*. E. coli aggregation and impaired cell division after terahertz irradiation. Sci Rep 2021;11(1):20464. doi:10.1038/s41598-021-99665-3, PMID:34650158.
[15] Demidova EV, Goryachkovskaya TN, Malup TK, Bannikova SV, Semenov AI, Vinokurov NA, *et al*. Studying the non-thermal effects of terahertz radiation on E. coli/pKatG-GFP biosensor cells. Bioelectromagnetics 2013;34(1):15–21. doi:10.1002/bem.21736, PMID:22674118.
[16] Bannikova S, Khlebodarova T, Vasilieva A, Mescheryakova I, Bryanskaya A, Shedko E, *et al*. Specific Features of the Proteomic Response of Thermophilic Bacterium Geobacillus icigianus to Terahertz Irradiation. Int J Mol Sci 2022;23(23):15216. doi:10.3390/ijms232315216, PMID:36499542.
[17] Bogomazova AN, Vassina EM, Goryachkovskaya TN, Popik VM, Sokolov AS, Kolchanov NA, *et al*. No DNA damage response and negligible genome-wide transcriptional changes in human embryonic stem cells exposed to terahertz radiation. Sci Rep 2015;5:7749. doi:10.1038/srep07749, PMID:25582954.
[18] Hoshina H. Order-disorder phase transition of cell membrane induced by THz irradiation. Sci Rep 2025;15(1):15091. doi:10.1038/s41598-025-99475-x, PMID:40301493.
[19] Hu E, Zhang Q, Shang S, Jiang Y, Lu X. Continuous wave irradiation at 0.1 terahertz facilitates transmembrane transport of small molecules. iScience 2022;25(3):103966. doi:10.1016/j.isci.2022.103966, PMID:35281735.
[20] Penkov NV. Terahertz spectroscopy as a method for investigation of hydration shells of biomolecules. Biophys Rev 2023;15(5):833–849. doi:10.1007/s12551-023-01131-z, PMID:37974994.
[21] Ma S, Ding P, Zhou Z, Jin H, Li X, Li Y. Terahertz Radiation Modulates Neuronal Morphology and Dynamics Properties. Brain Sci 2024;14(3):279. doi:10.3390/brainsci14030279, PMID:38539667.
[22] Butikova EA, Basov NV, Rogachev AD, Gaisler EV, Ivanisenko VA, Demenkov PS, *et al*. Metabolomic and gene networks approaches reveal the role of mitochondrial membrane proteins in response of human melanoma cells to THz radiation. Biochim Biophys Acta Mol Cell Biol Lipids 2025;1870(2):159595. doi:10.1016/j.bbalip.2025.159595, PMID:39842507.
[23] Klassen A, Faccio AT, Canuto GA, da Cruz PL, Ribeiro HC, Tavares MF, *et al*. Metabolomics: Definitions and Significance in Systems Biology. Adv Exp Med Biol 2017;965:3–17. doi:10.1007/978-3-319-47656-8_1, PMID:28132174.
[24] Silva RA, Pereira TCS, Souza AR, Ribeiro PR. (1)H NMR-based metabolite profiling for biomarker identification. Clin Chim Acta 2020;502:269–279. doi:10.1016/j.cca.2019.11.015, PMID:31778675.
[25] Demenkov PS, Ivanisenko TV, Kolchanov NA, Ivanisenko VA. ANDVisio: a new tool for graphic visualization and analysis of literature mined associative gene networks in the ANDSystem. In Silico Biol 2011-2 2012;11(3-4):149–161. doi:10.3233/ISB-2012-0449, PMID:22935968.
[26] Ivanisenko VA, Saik OV, Ivanisenko NV, Tiys ES, Ivanisenko TV, Demenkov PS, *et al*. ANDSystem: an Associative Network Discovery System for automated literature mining in the field of biology. BMC Syst Biol 2015;9(Suppl 2):S2. doi:10.1186/1752-0509-9-S2-S2, PMID:25881313.
[27] Ivanisenko VA, Demenkov PS, Ivanisenko TV, Mishchenko EL, Saik OV. A new version of the ANDSystem tool for automatic extraction of knowledge from scientific publications with expanded functionality for reconstruction of associative gene networks by considering tissue-specific gene expression. BMC Bioinformatics 2019;20(Suppl 1):34. doi:10.1186/s12859-018-2567-6, PMID:30717676.
[28] Ivanisenko TV, Saik OV, Demenkov PS, Ivanisenko NV, Savostianov AN, Ivanisenko VA. ANDDigest: a new web-based module of ANDSystem for the search of knowledge in the scientific literature. BMC Bioinformatics 2020;21(Suppl 11):228. doi:10.1186/s12859-020-03557-8, PMID:32921303.
[29] Ivanisenko TV, Demenkov PS, Kolchanov NA, Ivanisenko VA. The New Version of the ANDDigest Tool with Improved AI-Based Short Names Recognition. Int J Mol Sci 2022;23(23):14934. doi:10.3390/ijms232314934, PMID:36499269.
[30] Ivanisenko TV, Demenkov PS, Ivanisenko VA. An Accurate and Efficient Approach to Knowledge Extraction from Scientific Publications Using Structured Ontology Models, Graph Neural Networks, and Large Language Models. Int J Mol Sci 2024;25(21):11811. doi:10.3390/ijms252111811, PMID:39519363.
[31] Kulipanov GN, Bagryanskaya EG, Chesnokov EN, Choporova YY, Gerasimov VV, Getmanov YV. Novosibirsk Free Electron Laser-Facility Description and Recent Experiments. IEEE Trans Terahertz Sci Technol 2015;5(5):798–809. doi:10.1109/TTHZ.2015.2453121.
[32] Basov NV, Butikova EA, Sotnikova MA, Razumov IA, Sotnikova YS, Patrushev YV, *et al*. Features of sample preparation of cell culture samples for metabolomic screening by LC-MS/MS. J Pharm Biomed Anal 2026;267:117146. doi:10.1016/j.jpba.2025.117146, PMID:40972480.
[33] Patrushev Y V, Sotnikova YS, Sidel'nikov VN. A Monolithic Column with a Sorbent Based on 1-Vinyl-1,2,4-Triazole for Hydrophilic HPLC. Prot Met Phys Chem Surf 2020;56(1):49–53. doi:10.1134/S2070205119060248.
[34] Basov NV, Rogachev AD, Aleshkova MA, Gaisler EV, Sotnikova YS, Patrushev YV, *et al*. Global LC-MS/MS targeted metabolomics using a combination of HILIC and RP LC separation modes on an organic monolithic column based on 1-vinyl-1,2,4-triazole. Talanta 2024;267:125168. doi:10.1016/j.talanta.2023.125168, PMID:37708770.
[35] Kanehisa M, Sato Y, Kawashima M. KEGG mapping tools for uncovering hidden features in biological data. Protein Sci 2022;31(1):47–53. doi:10.1002/pro.4172, PMID:34423492.
[36] Wishart DS, Guo A, Oler E, Wang F, Anjum A, Peters H, *et al*. HMDB 5.0: the Human Metabolome Database for 2022. Nucleic Acids Res 2022;50(D1):D622–D631. doi:10.1093/nar/gkab1062, PMID:34986597.
[37] Mohamed A, Shah AD, Chen D, Hill MM. RaftProt V2: understanding membrane microdomain function through lipid raft proteomes. Nucleic Acids Res 2019;47(D1):D459–D463. doi:10.1093/nar/gky948, PMID:30329070.
[38] Shao X, Liao J, Li C, Lu X, Cheng J, Fan X. CellTalkDB: a manually curated database of ligand-receptor interactions in humans and mice. Brief Bioinform 2021;22(4):bbaa269. doi:10.1093/bib/bbaa269, PMID:33147626.
[39] Sherman BT, Hao M, Qiu J, Jiao X, Baseler MW, Lane HC, *et al*. DAVID: a web server for functional enrichment analysis and functional annotation of gene lists (2021 update). Nucleic Acids Res 2022;50(W1):W216–W221. doi:10.1093/nar/gkac194, PMID:35325185.
[40] Tong YB, Shi MW, Qian SH, Chen YJ, Luo ZH, Tu YX, *et al*. GenOrigin: A comprehensive protein-coding gene origination database on the evolutionary timescale of life. J Genet Genomics 2021;48(12):1122–1129. doi:10.1016/j.jgg.2021.03.018, PMID:34538772.
[41] Pang Z, Lu Y, Zhou G, Hui F, Xu L, Viau C, *et al*. MetaboAnalyst 6.0: towards a unified platform for metabolomics data processing, analysis and interpretation. Nucleic Acids Res 2024;52(W1):W398–W406. doi:10.1093/nar/gkae253, PMID:38587201.
[42] Wilmink GJ, Rivest BD, Ibey BL, Roth CL, Bernhard J, Roach WP. Quantitative investigation of the bioeffects associated with terahertz radiation. In: Optical Interactions with Tissues and Cells XXI. Proc of SPIE 2010;7562:75620L. doi:10.1117/12.844916.
[43] Echchgadda I, Cerna CZ, Sloan MA, Elam DP, Ibey BL. Effects of different terahertz frequencies on gene expression in human keratino-

cytes. Proc. SPIE 9321, Optical Interactions with Tissue and Cells XXVI 2015;9321:93210Q. doi:10.1117/12.2082542.
[44] Shatalova R, Gurova S, Revkova V, Ilina I, Sitnikov D. Influence of Powerful Non-Ionizing Terahertz Radiation on Healthy and Tumor Human Cells of Neural Origin. Med Radiol Radiat Saf 2021;66(5):5–10. doi:10.12737/1024-6177-2021-66-5-5-10.
[45] Tsurkan MV, Kudryavtsev IV, Serebryakova MK, Nesgovorova YS, Trulev AS, Nazarova IV, *et al*. The effect of radiation in the 0.05-1.2 THZ range on the mitochondrial membrane potential (In Russian). Scientific and Technical Bulletin of Information Technologies, Mechanics and Optics 2013;4(86):56–61.
[46] Naes SM, Ab-Rahim S, Mazlan M, Amir Hashim NA, Abdul Rahman A. Increased ENT2 expression and its association with altered purine metabolism in cell lines derived from different stages of colorectal cancer. Exp Ther Med 2023;25(5):212. doi:10.3892/etm.2023.11911, PMID:37123217.
[47] Shao S, Xu Q, Yu X, Pan R, Chen Y. Dipeptidyl peptidase 4 inhibitors and their potential immune modulatory functions. Pharmacol Ther 2020;209:107503. doi:10.1016/j.pharmthera.2020.107503, PMID:32061923.
[48] Mullen NJ, Singh PK. Nucleotide metabolism: a pan-cancer metabolic dependency. Nat Rev Cancer 2023;23(5):275–294. doi:10.1038/s41568-023-00557-7, PMID:36973407.
[49] Kameoka J, Tanaka T, Nojima Y, Schlossman SF, Morimoto C. Direct association of adenosine deaminase with a T cell activation antigen, CD26. Science 1993;261(5120):466–469. doi:10.1126/science.8101391, PMID:8101391.
[50] Wang J, Huang CL, Zhang Y. Complement C1q Binding Protein (C1QBP): Physiological Functions, Mutation-Associated Mitochondrial Cardiomyopathy and Current Disease Models. Front Cardiovasc Med 2022;9:843853. doi:10.3389/fcvm.2022.843853, PMID:35310974.
[51] Lei M, Zhang T, Lu X, Zhao X, Wang H, Long J, *et al*. Membrane-mediated modulation of mitochondrial physiology by terahertz waves. Biomed Opt Express 2024;15(7):4065–4080. doi:10.1364/BOE.528706, PMID:39022554.
[52] Lambert S, Vind-Kezunovic D, Karvinen S, Gniadecki R. Ligand-independent activation of the EGFR by lipid raft disruption. J Invest Dermatol 2006;126(5):954–962. doi:10.1038/sj.jid.5700168, PMID:16456534.
[53] Geng P, Ye F, Dou P, Hu C, He J, Zhao J, *et al*. HIF-1α-HPRT1 axis promotes tumorigenesis and gefitinib resistance by enhancing purine metabolism in EGFR-mutant lung adenocarcinoma. J Exp Clin Cancer Res 2024;43(1):269. doi:10.1186/s13046-024-03184-8, PMID:39343971.
[54] Lingwood D, Simons K. Lipid rafts as a membrane-organizing principle. Science 2010;327(5961):46–50. doi:10.1126/science.1174621, PMID:20044567.
[55] Sverdlov M, Shinin V, Place AT, Castellon M, Minshall RD. Filamin A regulates caveolae internalization and trafficking in endothelial cells. Mol Biol Cell 2009;20(21):4531–4540. doi:10.1091/mbc.e08-10-0997, PMID:19759182.
[56] Son JH, Cheon H. Toward cancer treatment using terahertz radiation: demethylation of cancer cells. Next-Generation Spectroscopic Technologies XII. Proc of SPIE 2020;11390:1139002. doi:10.1117/12.2557655.
[57] Cheon H, Yang HJ, Lee SH, Kim YA, Son JH. Terahertz molecular resonance of cancer DNA. Sci Rep 2016;6:37103. doi:10.1038/srep37103, PMID:27845398.
[58] Moran B, Silva R, Perry AS, Gallagher WM. Epigenetics of malignant melanoma. Semin Cancer Biol 2018;51:80–88. doi:10.1016/j.semcancer.2017.10.006, PMID:29074395.
[59] Sarkar D, Leung EY, Baguley BC, Finlay GJ, Askarian-Amiri ME. Epigenetic regulation in human melanoma: past and future. Epigenetics 2015;10(2):103–121. doi:10.1080/15592294.2014.1003746, PMID:25587943.
[60] Nikitkina AI, Bikmulina PY, Gafarova ER, Kosheleva NV, Efremov YM, Bezrukov EA, *et al*. Terahertz radiation and the skin: a review. J Biomed Opt 2021;26(4):043005. doi:10.1117/1.JBO.26.4.043005, PMID:33583155.